Natural Convection in Parabolic Enclosure Heated from Below

Dr. Ahmed W. Mustafa (Corresponding auther)

University of Tikrit, College of Engineering, Mechanical Engineering Department, Iraq Tel: 96-477-0071-7961 E-mail: ahmedweh@yahoo.com

Received: February 22, 2011

Accepted: March 13, 2011

doi:10.5539/mas.v5n3p213

Abstract

The effects of vertical parabolic walls on natural convection in a parabolic enclosure have investigated numerically in this paper. The bottom wall is heated isothermally, while the other vertical parabolic walls are maintained at constant cold temperature and the top wall is well insulated. The flow and temperature fields are studied numerically for three values (C = 0.1, 0.5, 1.0) of the parabolic equation constant. The laminar flow field is analyzed numerically by solving the steady, two-dimensional incompressible Navier-Stokes and energy equations. The Cartesian velocity components and pressure on a collocated (non-staggered) grid are used as dependent variables in the momentum equations, which discretized by finite volume method, body fitted coordinates are used to represent the complex parabolic wall geometry accurately, and grid generation technique based on elliptic partial differential equations is employed. **SIMPLE** algorithm is used to adjust the velocity field to satisfy the conservation of mass. The range of Rayleigh number is $(10^3 \le \text{Ra} \le 10^5)$ and Prandtl number is 0.7. The results show that the heat transfer rates decrease with increase the parabolic equation constant.

Keywords: Natural convection, Parabolic enclosure, Finite volume

1. Introduction

This study focuses on understanding of heat transfer by natural convection in parabolic enclosure as found in solar parabolic concentrators. Specifically, the effect of vertical parabolic walls of the enclosure on laminar natural convection is analyzed as a non-square enclosure heated from below.

Natural convection in differentially heated square enclosures has been studied extensively. De Val Davis (1983) obtained a benchmark numerical solution of buoyancy driven flow in a square cavity with vertical walls at different temperatures and adiabatic horizontal walls. De Val Davis and Jones (1983) presented a comparison of different contributed solutions to the same problem. These solutions covered the range of Rayleigh numbers between 10^3 to 10^6 . More recent contributions include a new benchmark quality solution by means of discrete singular convolution Wan etc. (2001), steady state and transient solutions using a fourth order momentum equation Bubnovich (2002), and a study of free convective laminar flow with and without internal heat generation in rectangular enclosures of different aspect rations at various angles of inclination Rahman and Sharif (2003).

Natural convection studies that include coordinate transformations include the works by Lee (1984) for convective fluid motion in a trapezoidal enclosure, Karyakin (1989) for prismatic enclosures of arbitrary cross section. Talabi and Nwabuko (1993) have studied the natural convection in parabolic enclosure numerically. The analytical model is consisting of a hot parabolic upper-wall, a cold horizontal base and an adiabatic vertical wall. Two cases of heat input from the parabolic upper-wall have been considered, isothermal condition on the hot wall, and constant heat-flux through the hot wall. The base and vertical walls are made isothermal and adiabatic, respectively Results show that in case of isothermal hot wall the heat transfer rate to the cold wall increases with increase in Grashof and Prandtl numbers. Diaz and Winston (2008) have analyzed the interaction of natural convection and surface radiation in two-dimensional parabolic cavities heated from below with insulated walls and flat top and bottom walls numerically. The numerical model based on finite differences is used to solve the mass, momentum, and energy equations. A coordinate transformation is used to map the parabolic shape into a rectangular domain where the governing equations are solved. The results show that surface radiation significantly changes the temperature distribution and local Nusselt number inside the parabolic enclosure. The aim of the present study is to investigate natural convection in a parabolic enclosure when bottom wall is heated isothermally and top wall is well insulated while two vertical parabolic walls are cooled by means of two constant temperature baths (see figure 1).

2. Problem Formulation

The treated problem is a two-dimensional parabolic enclosure with a height H and base wall of length L=H. The physical system considered in the present study is displayed in figure 1. The bottom wall is heated isothermally at temperature (T_h) and top wall is well insulated while two vertical wavy walls are cooled by means of two constant temperatures (T_c) . The fluid properties are assumed constant except for the density variation which is treated according to Boussinesq approximation. The viscous incompressible flow and the temperature distribution inside the cavity are described by the Navier–Stokes and the energy equations, respectively. The governing equations were transformed into dimensionless forms upon incorporating the following

$$X = \frac{x}{H}, \quad Y = \frac{y}{H}, \quad U = \frac{uH}{\alpha}, \quad V = \frac{vH}{\alpha}, \quad \theta = \frac{T - T_c}{T_h - T_c}, \quad P = \frac{pH^2}{\rho\alpha^2}, \quad \Pr = \frac{v}{\alpha}, \quad Ra = \frac{g\beta(T_h - T_c)H^3 \operatorname{Pr}}{v^2} \quad (1)$$

non-dimensional variables:

Where *X* and *Y* are the dimensionless coordinates measured along the horizontal and vertical axes, respectively, *u* and v being the dimensional velocity components along *x*- and *y* axes, and θ is the dimensionless temperature. The dimensionless forms of the governing equations under steady state condition are expressed in the following forms:

$$\frac{\partial U}{\partial X} + \frac{\partial V}{\partial Y} = 0 \tag{2}$$

$$\frac{\partial U^2}{\partial X} + \frac{\partial UV}{\partial Y} = -\frac{\partial P}{\partial X} + \Pr\left(\frac{\partial^2 U}{\partial X^2} + \frac{\partial^2 U}{\partial Y^2}\right)$$
(3)

$$\frac{\partial UV}{\partial X} + \frac{\partial V^2}{\partial Y} = -\frac{\partial P}{\partial Y} + \Pr\left(\frac{\partial^2 V}{\partial X^2} + \frac{\partial^2 V}{\partial Y^2}\right) + Ra\Pr\theta$$
(4)

$$\frac{\partial U\theta}{\partial X} + \frac{\partial V\theta}{\partial Y} = \left(\frac{\partial^2 \theta}{\partial X^2} + \frac{\partial^2 \theta}{\partial Y^2}\right)$$
(5)

3. Parabolic Walls

In order to simulate the vertical parabolic walls, the parabolic equation can be expressed as:-

$$X = +C\sqrt{Y} + 1 \quad (Right \ Wall), \qquad X = -C\sqrt{Y} \quad (Left \ Wall) \tag{6}$$

Where C is constant and has taken in this study for three values (0.1, 0.5, and 1).

3. Boundary Conditions

Boundary conditions can be summarized by the following equations:

Bottom Wall

$$U = V = 0, \quad \theta = 1, \quad \frac{\partial P}{\partial n} = 0$$

Top Wall

$$U = V = 0, \quad \frac{\partial \theta}{\partial n} = 0 \quad , \frac{\partial P}{\partial n} = 0$$

Left Wall

$$U = V = \theta = 0 \quad , \frac{\partial P}{\partial n} = 0$$

Right Wall

$$U = V = \theta = 0 \quad , \frac{\partial P}{\partial n} = 0$$

5. Numerical Method

The set of conservation equations (2-4) can be written in general form in Cartesian coordinates as

$$\frac{\partial(U\phi)}{\partial X} + \frac{\partial(V\phi)}{\partial Y} = \frac{\partial}{\partial X} \left(\Gamma \frac{\partial\phi}{\partial X} \right) + \frac{\partial}{\partial Y} \left(\Gamma \frac{\partial\phi}{\partial Y} \right) + S_{\phi}$$
(7)

Where Γ is the effective diffusion coefficient, ϕ is the general dependent variable, S_{ϕ} is the source term. The continuity equation (2) has no diffusion and source terms; it will be used to derive an equation for the pressure correction.

The grid generation scheme based on elliptic partial differential equations is used in the present study to generate the curvilinear coordinates. Equation (7) can be transformed from physical domain to computational domain according to the following transformation $\zeta = \zeta(x, y), \eta = \eta(x, y)$, the final form of the transformed equation can be written as:-

$$\frac{\partial}{\partial\varsigma}(\phi G_1) + \frac{\partial}{\partial\eta}(\phi G_2) = \frac{\partial}{\partial\varsigma} \left(\frac{\Gamma}{J} \left(\alpha \frac{\partial \phi}{\partial\varsigma} - \gamma \frac{\partial \phi}{\partial\eta} \right) \right) + \frac{\partial}{\partial\eta} \left(\frac{\Gamma}{J} \left(\beta \frac{\partial \phi}{\partial\eta} - \gamma \frac{\partial \phi}{\partial\varsigma} \right) \right) + JS_{\phi}$$
(8)

, G_1 and G_2 are the contravariant velocity components, J is the Jacobian of the transformation, on the computational plane, and α , β , γ are the coefficients of transformation. They are expressed as

$$G_{1} = U \frac{\partial Y}{\partial \eta} - V \frac{\partial X}{\partial \eta}, \qquad G_{2} = V \frac{\partial X}{\partial \varsigma} - U \frac{\partial Y}{\partial \varsigma}, \qquad J = \left(\frac{\partial X}{\partial \varsigma} \frac{\partial Y}{\partial \eta} - \frac{\partial Y}{\partial \varsigma} \frac{\partial X}{\partial \eta}\right)$$

$$\alpha = \left(\frac{\partial x}{\partial \eta}\right)^{2} + \left(\frac{\partial y}{\partial \eta}\right)^{2}, \qquad \gamma = \left(\frac{\partial x}{\partial \varsigma} \frac{\partial x}{\partial \eta}\right) + \left(\frac{\partial y}{\partial \varsigma} \frac{\partial y}{\partial \eta}\right), \qquad \beta = \left(\frac{\partial x}{\partial \varsigma}\right)^{2} + \left(\frac{\partial y}{\partial \varsigma}\right)^{2}$$
(9)

The transferred equation (8) is integrated over the control volume in the computation domain. The convective terms are discretized by using hybrid scheme, while the diffusion terms are discretized by central scheme. **SIMPLE** algorithm on a collocated nonorthogonal grid is used to adjust the velocity field to satisfy the conservation of mass. Since all variables are stored in the center of the control volume, the interpolation method is used in the pressure correction equation to avoid the decoupling between velocity and pressure as in Rhie and Chow (1983). In order to consider the effect of the cross derivatives and to avoid solving a nine diagonal matrix of the pressure-correction equation, the cross derivatives are calculated by the approximate method of Wang and Komori (2000). The resulting set of discretization equations are solved iteratively using the line-by-line procedure which uses the Tri-Diagonal Matrix Algorithm (TDMA). The convergence criterion is that the maximum residuals in all equations fall below 10^{-4} . For further information, numerical details can be found in Ferziger and Peric (1996).

6. Grid Independence Test

Computations have carried out for three selected grid sizes (i.e., 50×30 , 60×40 , and 70×50). Figure (2) shows local Nusselt number distribution along the hot bottom wall for Ra = 10^5 and C = 0.50. Results for the selected grid sizes show very good agreement with each other. Medium grid (60×40) is presented throughout this paper.

7. Validation

The model validation is an essential part of a numerical investigation. Hence, the present numerical results are compared with the numerical results of Tanmay Basak etc. (2009), which were reported for laminar natural convection heat transfer in a trapezoidal enclosure heated isothermally from below while the other vertical walls are maintained at constant cold temperature and the top wall is well insulated. The comparison is conducted while employing the following dimensionless parameters: $Ra = 10^5$, Pr = 0.7 and trapezoidal angle $\phi = 30^\circ$. Excellent agreement is achieved, as illustrated in figure (2), between the present results and the numerical results of Tanmay Basak etc. (2009) for the local Nusselt number distribution along the bottom wall.

8. Results and Discussion

Figure (4a-c) and (5a-c) illustrate the stream function and isotherm contours of the numerical results for $Ra = 10^3$ and 10^5 , respectively. The results are for Pr = 0. 7 and for three values of the parabolic equation constants (C =0.1, 0.5, and 1.0) when the bottom wall is heated isothermally and the side walls are cooled while the top wall is well insulated.

As expected due to the cold vertical parabolic walls, fluids rise up from middle portion of the bottom wall and flow down along the two vertical parabolic walls forming two symmetric rolls with clockwise and anti-clockwise rotations inside the cavity. At $Ra = 10^3$, the magnitudes of stream function are considerably lower and the heat

transfer is purely due to conduction. For (C=0.1), the temperature contours with $\theta = 0.1$ occur symmetrically near the side walls of the enclosure and the other temperature contours with $\theta \ge 0.2$ are smooth curves symmetric with respect to the vertical symmetric line as shown in figure (4a). On the other hand as the constant increases to (C=1.0) the temperature contours with $\theta \le 0.4$ occur symmetrically near the side walls of the enclosure and the other temperature contours with $\theta \ge 0.5$ are smooth curves symmetric with respect to the vertical symmetric line as shown in figure (4c), this is due to the increase of the area of the vertical cold walls.

At larger Ra = 10^5 , the effect of buoyancy force is stronger compared to viscous forces and the intensity of fluid motion has been increased as indicated by larger magnitudes of streamfunctions (figure (5a-c)). The enhanced convection causes larger heat energy to flow from the bottom wall to the top portion of the vertical wall and a large regime of top portion of the cavity remains at uniform temperature for C=0.5 and C =1. It is interesting to observe that the stratification zone of temperature at the central vertical line near the bottom wall is suppressed for Ra = 10^5 due to enhanced convection whereas the stratification zone is larger for Ra = 10^3 . It may be noted that the stratification zone of temperature at bottom is thicker for C = 0.1 due to less intense circulation near the top portion of the cavity. It is also observed that the isotherms are compressed strongly towards the side walls for Ra = 10^5 especially with C = 0.5 and C = 1.0 as shown in (figure (5b-c)). The isotherms with $\theta \le 0.4$ are compressed near the side walls of the enclosure for C = 0.1, 0.5, and 1. It is also observed that isotherms for C = 1.0 are more distorted (figure (4c)) compared to C = 0.1 (figure (4a)) due to the extension of circulation in the whole enclosure.

Figure (6) illustrates the local Nusselt number verses distance for the bottom wall, for Pr = 0.7 and $Ra = 10^5$ and for three values of the parabolic equation constants (C =0.1, 0.5, and C = 1). It is observed that the heat transfer rate is maximum near the edge of the wall and the rate is minimum near the center of the wall for all constants (C = 0.1, 0.5, and 1). It is also interesting to observe that the heat transfer rates (Nu) for (C = 0.5 and C = 1) are smaller that heat transfer rates (Nu) for C = 0.1 due to highly compressed isotherms as seen from figure (5a). Figure (7) illustrates that average Nusselt number (Nua) increases with Rayleigh number for all the three values of constants (C). It is observed that heat transfer rate is largest for (C = 0.1), this may be explained based on local Nusselt number plots as shown in figure (6).

9. Conclusion

The finite volume method with collocated grid is used to analyze the natural convection in parabolic enclosure. The heat transfer rates have analyzed with local and average Nusselt numbers for the bottom wall of the enclosure. The results show that the local heat transfer rate is larger for the small value of the parabolic equation constant (C =0.1) and also the average heat transfer rate is larger for C =0.1.

References

Bubnovich V., Rosas C., Santander R., and Caceres G. (2002). Computation of Transient Natural Convection in a Square Cavity by an Implicit Finite-Difference Scheme in Terms of the Stream Function and Temperature, Numer. *Heat Transfer A*, vol. 42, pp. 401–425, 2002.

De Vahl Davis G. (1983). Natural Convection of Air in a Square Cavity: A Bench Mark Numerical Solution, *Int. J. Num. Meth. Fluids*, vol. 3, pp. 249–264, 1983.

De Vahl Davis G. and Jones I. P. (1983). Natural Convection in a Square Cavity: A Comparison Exercise, *Int. J. Num. Meth. Fluids*, vol. 3, pp. 227–248, 1983.

Diaz G. and Winston R. (2008). Effect of surface radiation on natural convection in parabolic enclosure, *numerical heat transfer*, part a 53, 891-906, 2008.

Ferziger, J.H. and Peric, M. (1996). Computational Methods for Fluid Dynamics, Springer 1996.

Karyakin Y. E. (1989). Transient Natural Convection in Prismatic Enclosures of Arbitrary Cross-Section, Int. J. Heat Mass Transfer, vol. 32, 6, 1095–1103, 1989.

Lee T. S. (1984). Computational and Experimental Studies of Convective Fluid Motion and Heat Transfer in Inclined Non-Rectangular Enclosures, *Int. J. Heat Fluid Flow*, 5, 29–36, 1984.

Rahman M. and Sharif M. A. R. (2003). Numerical Study of Laminar Natural Convection in Inclined Rectangular Enclosures of Various Aspect Ratios, Numer. *Heat Transfer A*, vol. 44, pp. 355–373, 2003.

Rhie, C. M., and Chow, W. L. (1983). Numerical Study of the Turbulent Flow Past an Airfoil with Trailing Edge Separation, *AIAA Journal*, 21, 1525-1532, 1983.

Talabi S.O., and Nwabuko U. (1993). Numerical solution of natural convective heat transfer in parabolic enclosures, *Int. J. Heat Mass Transfer*, 36, 17, 4275–4281, 1993.

Tanmay Basak, S.Roy, I.Pop. (2009). Heat flow analysis for natural convection within trapezoidal enclosures based on heatline concept, *Int. J. Heat Mass Transfer* 52, 2471–2483, 2009.

Wan D. C., Patnaik B. S. B., and Wei G. W. (2001). A New Benchmark Quality Solution for the Buoyancy-Driven Cavity by Discrete Singular Convolution, Numer. *Heat Transfer B*, vol. 40, pp. 199–228, 2001.

Wang Y. and Komori S. (2000). On the improvement of the SIMPLE-like method for flows with complex geometry, *Heat and Mass Transfer* 36, 71-78, 2000.

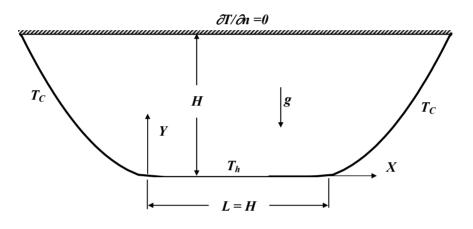


Figure 1. Schematic diagram of the physical system

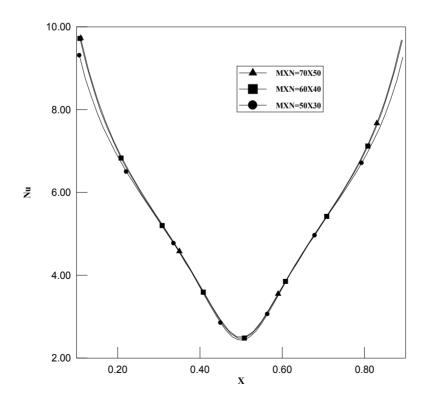


Figure 2. Grid independence test for local Nusselt number for $Ra = 10^5$, C = 0.5

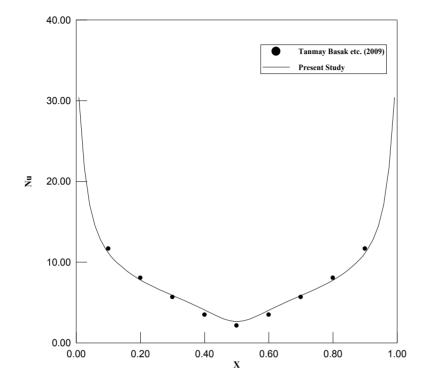


Figure 3. Comparison of the present study with the result of Tamnay Basak etc.(2009) for local Nusselt Number on the bottom wall of trapezoidal enclosure for Ra =10⁵, Pr = 0.7 and trapezoidal angle (ϕ =30°)

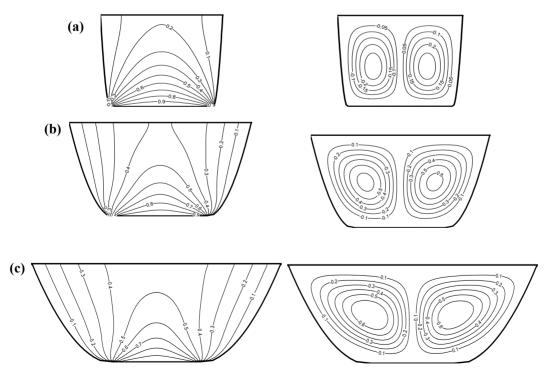


Figure 4. Isotherms Contours (left) and Streamlines contour (right) for Ra= 10^3 , Pr = 0.7 and for (a) C=0.1 (b) C =0.5, and (c) C =1.0

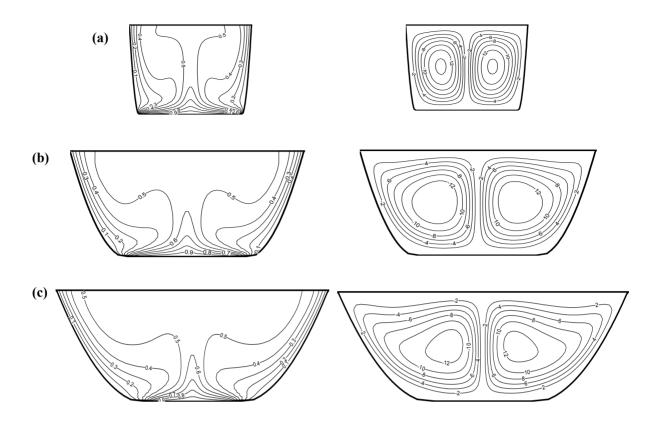


Figure 5. Isotherms Contours (left) and Streamlines contour (right) for Ra= 10^5 , Pr = 0.7 and for (a) C=0.1 (b) C =0.5, and (c) C =1.0

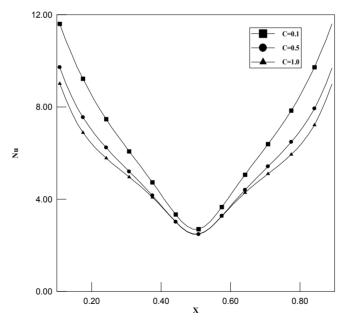


Figure 6. Local Nusselt number on the bottom wall of the enclosure fore $Ra = 10^5$, Pr=0.7 and for three different values of the constant C

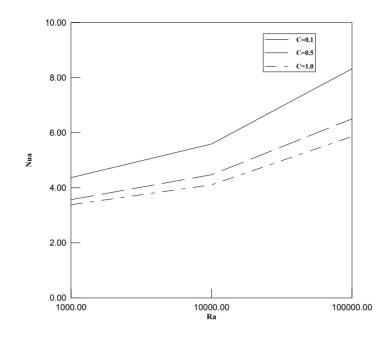


Figure 7. Average Nusselt number versus Rayleigh number for three different values of the constant C